HHS Public Access

Author manuscript

Nat Chem. Author manuscript; available in PMC 2020 November 18.

Published in final edited form as:

Nat Chem. 2020 July ; 12(7): 638–646. doi:10.1038/s41557-020-0460-1.

Aerobic Radical Polymerization Mediated by Microbial Metabolism

Gang Fan[1,2], **Austin J. Graham**[1,2], **Jayaker Kolli**[1], **Nathaniel A. Lynd**[1,2], **Benjamin K. Keitz**[1,2]

[1]McKetta Department of Chemical Engineering, University of Texas at Austin, Austin, TX 78712, USA

[2]Center for Dynamics and Control of Materials, University of Texas at Austin, Austin, TX 78712, USA

Abstract

Performing radical polymerizations under ambient conditions is a significant challenge because molecular oxygen is an effective radical quencher. Here we show that the facultative electrogen *Shewanella oneidensis* can control metal-catalyzed living radical polymerizations under apparent aerobic conditions by first consuming dissolved oxygen via aerobic respiration, then directing extracellular electron flux to a metal catalyst. In both open and closed containers, *S. oneidensis* enabled living radical polymerizations without requiring the pre-removal of oxygen. Polymerization activity was closely tied to *S. oneidensis* anaerobic metabolism through specific extracellular electron transfer (EET) proteins and was effective for a variety of monomers using low (ppm) concentrations of metal catalysts. Finally, polymerizations survived repeated challenges of oxygen exposure and could be initiated using lyophilized or spent (recycled) cells. Overall, our results demonstrate how the unique ability of *S. oneidensis* to use both oxygen and metals as respiratory electron acceptors can be leveraged to address salient challenges in polymer synthesis.

Introduction

Radical-based reactions, including radical polymerizations, are inhibited in the presence of molecular oxygen[1,2]. Thus, controlled radical polymerizations require strictly anoxic conditions prior to initiation. Inspired by oxygen-consuming reactions in biology, several recent reports have shown that enzymatic reactions, such as the oxidation of β-D-glucose to D-glucono-δ-lactone via glucose oxidase, can rapidly deplete dissolved oxygen prior to reversible addition-fragmentation chain transfer (RAFT)[3,4] and atom transfer radical polymerization (ATRP)[5-7]. Similarly, combinations of enzymes such as glucose oxidase and horseradish peroxidase can enable radical polymerizations that require the presence of

Correspondence and requests for materials should be addressed to B.K.K. keitz@utexas.edu.

Author Contributions: G.F., A.J.G., N.A.L., and B.K.K. designed research; G.F., A.J.G., and J.K. performed research; N.A.L. contributed new reagents/analytic tools; G.F., A.J.G., N.A.L., and B.K.K. analyzed data and wrote the paper.

Data Availability. Raw data supporting the findings in this study are available through the Texas Data Repository (https://doi.org/10.18738/T8/KHF1AY)

Competing Interests: The authors declare no competing interest.

oxygen to generate the radical initiator[8]. These and other recent advances allow some living radical polymerizations to be run in open containers under ambient conditions[9-12]. However, the majority of polymerization methods relying on *in situ* oxygen depletion require sacrificial reagents, produce strong oxidants, and/or are restricted to specific catalysts and monomers.

Given the inspiration behind the use of glucose oxidase, we predicted that whole-cell aerobic respiration could similarly deplete dissolved oxygen prior to initiating radical polymerization (Figure 1). Towards this goal, we recently reported that the facultative electrogen *Shewanella oneidensis* (wild type, MR-1) can drive ATRP under anaerobic conditions by directing metabolic electron flux via its extracellular electron transfer (EET) machinery to Cu-based catalysts[13]. Because of its respiratory plasticity, we hypothesized that *S. oneidensis* could metabolically control living radical polymerizations under ambient conditions by first consuming dissolved oxygen, then directing EET flux to a metal polymerization catalyst (Figure 1). Here, we demonstrate that *S. oneidensis* enables ATRP under aerobic conditions using a variety of monomers and metal catalysts at low (ppm) concentrations. Aerobic polymerizations suppressed background radical reactions, could be run in open or shaking containers, and accentuated metabolic and genotypic differences between *S. oneidensis* strains. Finally, aerobic polymerizations produced homopolymers and block copolymers with well-controlled molecular weights at rates comparable to other polymerization methodologies and could be initiated using lyophilized or spent cells. Overall, our results demonstrate how the unique metabolic capabilities of *S. oneidensis* effectively combine the advantages of enzymatic oxygen depletion and Activator Regenerated by Electron Transfer (ARGET) ATRP to yield well-defined synthetic polymers under ambient conditions.

Results

S. oneidensis **consumes dissolved oxygen and activates EET flux to the metal polymerization catalyst**

In order to verify that S. oneidensis could create the anaerobic environment necessary for radical polymerization, we first measured dissolved oxygen depletion in *S. oneidensis* cultures under standard growth and polymerization conditions. In defined media (*Shewanella* Basal Medium, Supplementary Table 2) at an inoculation cell density of OD_{600} = 0.2, *S. oneidensis* MR-1 growing on lactate consumed dissolved oxygen within minutes (Figure 2a). Next, we examined oxygen consumption under typical polymerization conditions. We previously showed that polymerization mixtures containing monomer ($OEOMA_{500}$ [OEOMA = oligo(ethylene oxide) methyl ether methacrylate]), initiator (HEBIB [HEBIB = 2-hydroxyethyl 2-bromoisobutyrate]), lactate as the primary carbon source, fumarate as the primary electron acceptor, and metal catalyst (Cu(II)-TPMA [TPMA = Tris(2-pyridylmethyl)amine]) inhibit bacterial growth, although cells remain viable[13]. Nevertheless, cultures containing polymerization components also showed rapid oxygen depletion, albeit at a slower rate. Together, these results confirm that high densities of *S. oneidensis* cells quickly consume dissolved oxygen during growth in defined media and under typical polymerization conditions.

Having confirmed that oxygen can be readily removed from *S. oneidensis* polymerization cultures, we next assessed the general feasibility of aerobic polymerizations. Below, aerobic conditions refer to polymerizations using aerobically pre-grown cells with no steps taken to remove oxygen. Anaerobic conditions refer to polymerizations involving anaerobically pre-grown cells performed in the absence of oxygen. In a typical polymerization reaction, *S. oneidensis* cells from stationary-phase pre-growth were inoculated into a polymerization mixture containing monomer ($OEOMA_{500}$), initiator (HEBIB), lactate as the primary carbon source, fumarate as the primary anaerobic electron acceptor, and metal catalyst (Cu-TPMA). In a closed vessel with no additional steps taken to remove oxygen, a polymerization mixture containing aerobically pre-grown *S. oneidensis* at an inoculation density of OD_{600} = 0.2 showed near quantitative monomer conversion (^{1}H NMR spectroscopy) after two hours. This result confirmed that polymerization was possible under ambient conditions, but we wished to uncover the specific role of each reaction component. For example, we previously observed a catalyst-free background polymerization that proceeded to ca. 40% $OEOMA_{500}$ conversion over a 24 h period under anaerobic conditions[13]. Under aerobic conditions, all polymerization components including monomer, initiator, metal catalyst, and actively respiring *S. oneidensis* cells were required for monomer conversion (Figure 2b). Neglecting any of these components resulted in significantly attenuated monomer conversion or no measurable activity in the case of *S. oneidensis* supernatant or cell-free negative controls. Although some background polymerization activity was observed in the absence of metal catalyst or initiator, these levels were lower than under comparable anaerobic conditions[13]. During anaerobic polymerizations, we previously observed that lysed cells (both *S. oneidensis* MR-1 and *Escherichia coli* MG1655) could initiate significant monomer conversion via the release of cytosolic reductants. In contrast, aerobic conditions suppressed background polymerization activity from lysed cells (Figure 2c). These results show that in the absence of an active mechanism to remove dissolved oxygen (i.e., aerobic respiration), initiation caused by adventitious radicals or uncontrolled reduction of the Cu catalyst is inhibited.

In general, aerobic polymerizations in sealed vessels exhibited first-order kinetics, indicating effective control over radical concentration and allowing us to quantify polymerization rates (Supplementary Fig. 1). We measured polymerization rates of $OEOMA_{500}$ under aerobic conditions as a function of starting inoculum size (OD_{600}) and found a linear dependence above a threshold OD_{600} = 0.1 (Figure 2d). Below this cell population size, aerobic respiration can presumably not compensate for oxygen diffusion in order to create the anaerobic environment necessary for polymerization. Under anaerobic conditions (including pre-growth), polymerization rate was also proportional to the initial inoculum size and could be measured as low as OD_{600} = 0.004 (Supplementary Fig. 1). Thus, when normalized to initial cell population, aerobic polymerization rate constants were lower than those under anaerobic conditions, but still characteristic of a controlled polymerization. Notably, polymerizations run in completely open containers were also successful, with measured rate constants consistent with reactions in closed vessels (Supplementary Fig. 3). Furthermore, at higher cell densities, polymerizations were also tolerant to increased oxygen mass transfer, as indicated by successful polymerizations in tubes shaking at 100 RPM (Supplementary Fig. 4). Overall polymerization rate constants using Cu(II)-TPMA and *S. oneidensis* MR-1 under aerobic conditions were largely comparable to rates using glucose oxidase and horseradish peroxidase (~1.5 h^{-1} vs 0.56–5.9 h^{-1} respectively) but at lower catalyst concentrations (~20 ppm vs 100–1000 ppm relative to monomer)[6].

EET-controlled polymerization activity varies with metal catalyst and ligand environment

The polymerization rate of ATRP can be altered through the use of different Cu ligands or by using different metal catalysts. Under both aerobic and anaerobic conditions, polymerization rate could be varied over several orders of magnitude by changing the ligand for Cu (Figure 3b,c). Specifically, rates decreased in the order TPMA>bpy>Me_6TREN [bpy = 2,2'-bipyridine, Me_6TREN = Tris[2-(dimethylamino)ethyl]amine]. In an electrochemical cell under aqueous conditions, Me_6TREN previously displayed a faster polymerization rate compared to TPMA[14-16]. Our results indicate that in addition to affecting reduction potential, deactivation rate, and disproportionation propensity, the ligand environment around Cu may also influence its interaction with *S. oneidensis*' EET machinery. Therefore, we examined the specific role of MtrC, one of the terminal reductases that allows *S. oneidensis* to use metals and metal oxides as electron acceptors (Figure 3a)[17,18]. Consistent with our previous study, a *S. oneidensis* strain lacking *mtrC* (Δ*mtrC*Δ*omcA*) showed significantly attenuated $OEOMA_{500}$ polymerization rates for all Cu catalysts tested (Supplementary Fig. 5). Residual polymerization activity in the Δ*mtrC*Δ*omcA* strain is likely due to the presence of other EET pathways (i.e., MtrDEF), which may also mediate Cu(II) reduction. Indeed, using $OEOMA_{300}$ as monomer, additional *S. oneidensis* EET knockouts showed aerobic polymerization activity proportional to the number of cytochrome deletions (Supplementary Fig. 6). Together, these results highlight the extensive chemical (ligand structure) and biological (genotype) tools available for controlling polymerization activity under aerobic conditions.

Because our polymerization is driven by EET flux to a metal catalyst, we predicted that other metals besides Cu would show appreciable polymerization activity under both anaerobic and aerobic conditions. Indeed, metal catalysts comprised of Fe[19,20], Co[21,22], Ni[23,24], and Ru[25] have all been reported to exhibit ATRP-like activity. Although alternative metal catalysts are generally less active than Cu, they are potentially advantageous due to their lower toxicity. Furthermore, many of these metals can support *S. oneidensis* growth or lie within the redox range of its outer membrane cytochromes[17,26-28]. As predicted, we measured significant polymerization activity, relative to metal-free background controls, under anaerobic conditions for a variety of metal salts at low concentration (2 μM) using EDTA [EDTA = Ethylenediaminetetraacetic acid] as ligand (Figure 4a). Similar to the case with Cu catalysts, the Δ*mtrC*Δ*omcA* strain and *E. coli* MG1655 consistently showed reduced activity relative to *S. oneidensis* MR-1 for most of the metals tested (Supplementary Figs. 7-9). Next, we examined the activity of other metal complexes including cyanocobalamin, $[Co(en)_3](NO_3)_3$ [en = ethylenediamine], $FeC_6H_5O_7$ (citrate), $[Ni(en)_3]Cl_2$, and $[Ru(bpy)_3]Cl_2$ (Figure 4b). With the exception of $[Co(en)_3](NO_3)_3$, all complexes showed activity above background levels in the presence of *S. oneidensis* under anaerobic conditions. Subsequently, we measured the polymerization activity of several alternative metal catalysts under aerobic conditions. Only a handful of alternative metal catalysts at low concentration showed appreciable activity under these more challenging conditions, with stark differences in polymerization rate between *S. oneidensis* MR-1 and the Δ*mtrC*Δ*omcA* knockout (Figure 4c). Consistent with previous reports[19,20], aerobic polymerization rates for $FeCl_3$, cyanocobalamin, and $CuSO_4$ were lower compared to optimized Cu-based catalysts. Although fewer metals were active under aerobic conditions, our results indicate that additional ligand optimization or increasing catalyst concentration could significantly improve activity, as was the case when Cu(II)-EDTA was replaced with Cu(II)-TPMA[13].

EET-controlled polymerization is effective for a variety of monomers

Next, we evaluated monomer scope and polymer properties under both anaerobic and aerobic conditions (Table 1). Cells were generally tolerant to many of the monomers tested, with minimal effects on viability (Supplementary Fig. 10). As a result, many of these monomers were amenable to microbial polymerization under both anaerobic and aerobic conditions. Even water-insoluble and toxic monomers, such as styrene[29], could be polymerized via emulsion polymerization, albeit with low yield (Supplementary Fig. 11). At low concentrations of Cu(II)-TPMA (2 μM) and anaerobic conditions, theoretical molecular weights were significantly higher than predicted, likely due to inefficient initiation or catalyst deactivation (Supplementary Table 4). However, increasing the Cu concentration to 10 μM (~100 ppm relative to monomer) and using a more water-soluble initiator [poly(ethylene glycol) methyl ether 2-bromoisobutyrate, PEGBIB] brought theoretical and predicted molecular weights into closer alignment while maintaining narrow polydispersities and having a minimal effect on cell viability (Table 1, Supplementary Fig. 12). Overall trends in polymer molecular weight and polydispersity generally extended to aerobic conditions. For example, water-soluble monomers including $OEOMA_{300/500}$, HEMA [HEMA = (hydroxyethyl)methacrylate], and NIPAM [NIPAM = *N*-isopropylacrylamide] yielded well-defined polymers near the targeted molecular weight under aerobic conditions. GPC traces for these polymers were also comparable to those from polymerizations conducted under anaerobic conditions (Supplementary Fig. 13). Polymer characteristics, such as polydispersity, were generally comparable to polymers prepared through traditional aqueous ATRP[6,8]. Narrow polydispersities (Đ~1.1) for poly($OEOMA_{300}$) were also obtained when $FeCl_3$ and cyanocobalamin were used as catalysts under aerobic conditions, although molecular weight was significantly higher than predicted (Supplementary Fig. 14). Finally, using Cu(II)-TPMA, water-insoluble monomers, including styrene and MMA [MMA = methyl methacrylate], only yielded small amounts of polymer with non-ideal GPC traces under aerobic conditions. We attribute the performance of these monomers to a combination of poor solubility, the absence of surfactants in our media, and cellular toxicity. Nevertheless, our results indicate that *S. oneidensis* mediated polymerization is generally effective for a variety of monomers under both anaerobic and aerobic conditions.

Based on the range of different monomers amenable to polymerization, we next explored the synthesis of block copolymers (Figure 5a). Using our standard aerobic conditions, $OEOMA_{300}$ was added to a polymerization mixture containing *S. oneidensis*. After 2 hours, a second monomer (HEMA) was added to form the block copolymer. GPC traces following polymer isolation revealed an increase in molecular weight relative to $OEOMA_{300}$ homopolymer and a final PDI = 1.33 (Figure 5b). Based on the success of block copolymer synthesis, we predicted that chain extension could also occur following exposure of the polymerization mixture to oxygen. Indeed, previous reports using enzymatic depletion of dissolved oxygen showed that polymerization can be stopped and restarted in the presence of oxygen[8]. Similarly, we found that aerating by bubbling air through a monomer-containing microbial culture stopped polymerization, but that polymerization proceeded at similar rates when aeration ceased (Figure 5c). The resumption of polymerization was also associated with increased polymer molecular weight (Figure 5d, Supplementary Fig. 15). Together, these results demonstrate that our system can survive multiple oxygen challenges and can serve as a general platform for the synthesis of more advanced polymer architectures.

Polymerization activity is coupled to media formulation through *S. oneidensis* metabolism

We previously established that polymerization activity is dependent on EET flux, which can be altered using different carbon sources[13]. Under aerobic conditions, activity should also depend on cellular respiration since this consumes dissolved oxygen and is a prerequisite for radical propagation. Thus, we explored the relationship between cellular respiration and polymerization activity by changing nutrient availability and employing different buffers. Consistent with the important role of functional metal reduction pathways, cells pre-grown in media lacking iron showed reduced polymerization activity. Although we couldn’t distinguish this effect from a general growth defect, it suggests that *S. oneidensis* was unable to obtain enough iron to construct functional components of the Mtr pathway (e.g., hemes) (Supplementary Fig. 16). Using anaerobically pre-grown cells and polymerization conditions, the buffer had a minimal effect on polymerization activity (Supplementary Fig. 17). During anaerobic growth, *S. oneidensis* expresses a proteome optimized for metal reduction, including the Mtr pathway[26,30]. In contrast to our anaerobic results, aerobic polymerizations were highly dependent on the choice of microbial growth media (Supplementary Fig. 17). Polymerizations run in HEPES and PBS buffers showed reduced activity relative to *Shewanella* basal media (SBM) with casamino acids. We observed a similar decrease in aerobic polymerization rates when casamino acids were removed from SBM. Altogether, these results indicate that polymerization activity is closely coupled to aerobic and anaerobic respiratory pathways.

Lyophilized and spent cells can be employed as simple and regenerable polymerization reagents

A relative disadvantage of our aerobic polymerization is that it requires a pre-culturing step to obtain a sufficient density of *S. oneidensis* cells. To potentially streamline this protocol, we investigated whether lyophilized *S. oneidensis* cell powder could be directly added to an aerobic polymerization mixture (Figure 6a). Using $OEOMA_{500}$ as monomer, lyophilized cells showed comparable aerobic polymerization activity to pre-cultured cells, but required a higher initial cell density (Figure 6b). We also found that viable, spent cells could be collected from the polymerization mixture via centrifugation and reused for additional reactions after a short recovery period (~6 h) and supplying fresh reagents. Reactions conducted in this manner showed comparable polymerization kinetics and polymer properties to those using freshly cultured cells (Figure 6c). Combined, these results demonstrate that our polymerization is effective without prior microbiology experience and that simple bioreactor designs, such as fermenters, could potentially be adapted for polymerization. Finally, the use of lyophilized cells and the ability to survive repeated challenges with oxygen highlight the robustness and potential scalability of our polymerization platform.

Discussion

We showed that *S. oneidensis* enables aerobic radical polymerizations by first consuming dissolved oxygen via aerobic respiration, then activating an ATRP catalyst through extracellular electron transfer (EET). While a number of recent studies have performed radical polymerizations in the presence of living systems[31-33], our work demonstrates that microbial metabolism can be coopted to rigorously control synthetic polymerizations under benchtop conditions. Aerobic polymerizations involving *S. oneidensis* compare favorably to alternative oxygen-tolerant polymerization methodologies. Photoredox catalysts (both organic and inorganic) are effective in organic solvents, but normally require small volumes and higher catalyst concentrations to account for oxygen depletion[9,34], although ppm levels can be used in some cases[35]. However, these systems are advantageous for monomers with limited aqueous solubility, such as styrene and MMA, and are not limited by the need for aqueous conditions. Enzymatic methods for *in situ* oxygen consumption are the most comparable to our platform since they are also generally limited to physiological temperatures and pH. As mentioned above, the use of glucose oxidase for oxygen depletion has been highly successful for both RAFT and ATRP, producing polymers with controlled molecular weights and narrow polydispersities[3,4,6,8,11]. In contrast to our system, enzymatic polymerizations are not limited by potential concerns over cell viability. However, the direct production of hydrogen peroxide via glucose oxidase can be problematic for ATRP since the simultaneous presence of reduced metals can result in the creation of reactive oxygen species[6]. Thus, sacrificial reagents (i.e., pyruvate) or additional enzymes are typically required to sequester hydrogen peroxide. Facultative bacteria, including *S. oneidensis*, are specifically adapted for transitioning between aerobic and anaerobic environments. A carbon source is required for polymerization, but this also contributes to biomass production and cellular respiration. Most importantly, the living nature of bacteria enables unique tunability and optimization through microbial engineering techniques (e.g., metabolic pathway engineering, protein evolution, media optimization, etc.) that is unavailable to other aerobic polymerization methods.

In general, we found that polymer molecular weight and polydispersity control using aerobic conditions, Cu-TPMA, and *S. oneidensis* MR-1 were comparable to polymers prepared using alternative aqueous ATRP strategies[36]. A variety of monomers could be successfully polymerized and more advanced architectures including block copolymers were also prepared. Polymer chain extension was also possible after challenging the culture with oxygen, suggesting our polymerizations are robust toward repeated oxygen exposure. These results are notable because there are a number of challenges inherent to aqueous ATRP, especially under aerobic conditions. As mentioned above, oxygen-tolerant ATRP using glucose oxidase produces reduced metals and strong oxidants, which can result in Fenton chemistry. Hydrogen peroxide is also a natural byproduct of aerobic respiration. Indeed, *S. oneidensis* cultures produce hydrogen peroxide, especially after repeatedly transitioning from aerobic to anaerobic environments[37]. We speculate that reactive oxygen species generated through these processes may contribute to the relatively high polydispersities we measured for some monomers. Our initiator-free controls (Figure 2b) allow us to estimate the maximum potential contribution of uncontrolled polymerization as ~20% monomer conversion. Despite this, aerobic conditions eliminated a variety of other background polymerization processes relative to our previous anaerobic conditions. For example, we found that catalyst-free controls generated <10% monomer conversion under aerobic conditions, while ~40% conversion was observed under comparable anaerobic conditions[13]. Similarly, aerobic conditions eliminated polymerizations caused by the release of adventitious reductants during cell lysis. A variety of processes in addition to reactive oxygen species could erode control over the polymerization. For example, *S. oneidensis* produces flavins[38], which exhibit polymerization activity upon light irradiation[39]. In our previous work, we measured similar polymerization rates in *S. oneidensis* MR-1 and a flavin exporter knockout strain (Δ*bfe*), suggesting flavins are not significant contributors to polymerization activity[13]. However, we have not explored supplementation with exogenous flavins and the overall effect of flavins on background polymerization, as well as Cu(II) reduction, remains unexplored. Finally, free heme, as well as protein-bound heme (e.g., hemoglobin) are also effective ATRP catalysts and may contribute to background polymerization in our system[19]. Thus, MtrC, which contains at least one solvent-exposed heme[40], could potentially catalyze polymerization in the absence of an exogenous metal catalyst. Overall, the significant reduction of background processes in ambient conditions indicates that controlled, continuous electron flux to the catalyst through EET is the predominant source of polymerization activity. Nevertheless, isolating and eliminating competing background radical polymerizations will be essential to improving the synthesis of well-defined polymers using *S. oneidensis*.

The chemical mechanism of ATRP may also contribute to deviations from target molecular weights and narrow polydispersities. The equilibrium constant (K_{ATRP}) between Cu(I) and Cu(II) in water is particularly large, which accelerates the rate of polymerization but can also lead to halide dissociation and early polymer chain termination[41,16]. We observed this effect in our system at high optical densities (OD_{600} ~ 0.2, Supplementary Fig. 1) under anaerobic conditions where high EET flux presumably results in a large Cu(I) concentration that pushes K_{ATRP} even further toward Cu(II) and radical generation. This results in polymerization kinetics that deviate from first-order and monomer conversion that prematurely ceases due to chain end termination. This mechanism also helps explains why fumarate is beneficial as the primary anaerobic electron acceptor. Our standard Cu(II) concentration (2–10 μM) is too low to support anaerobic cell growth. Thus, the presence of fumarate ensures that *S. oneidensis* can readily transition from aerobic to anaerobic respiration while maintaining the metabolic flux necessary for polymerization. Aerobic polymerizations still occur in the absence of fumarate but are less controlled (Supplementary Fig. 18). We hypothesize that the loss of control occurs because a second function of fumarate is to divert respiratory flux from the EET pathways responsible for Cu(II) reduction. Reducing EET flux potentially decreases the concentration of Cu(I), K_{ATRP}, and the frequency of side reactions that lead to chain end termination. Thus, including fumarate results in a more controlled polymerization. To counteract the large aqueous K_{ATRP}, higher salt (NaCl, etc.) concentrations are typically required in aqueous polymerizations, including those performed with glucose oxidase, to suppress halide dissociation and chain termination.

We did not include extra salts in our *S. oneidensis* polymerization cultures but note that this species is halotolerant up to 0.2 M NaCl. This tolerance exceeds the NaCl concentrations (>10 mM) typically used in aqueous ATRP[36]. Additionally, many *Shewanella* species are isolated from marine environments and readily tolerate increased NaCl concentrations up to 2 M[42,43], making salt addition a potentially viable strategy for increasing polymerization control in our system. Finally, the use of less active metals, which we showed exhibit some activity under aerobic conditions, may also be important for increasing polymerization control.

Polymerization activity was highly dependent on both aerobic and anaerobic cellular metabolism. Specifically, we found that a critical population size (OD_{600} ~ 0.1) was necessary to counteract oxygen diffusion and enable radical polymerizations under aerobic conditions. Live cells also allowed polymerizations to survive repeated challenges with oxygen, facilitating polymer chain extension even after oxygen exposure. In contrast, heat-killed cells showed no polymerization activity while *S. oneidensis* grown in non-optimal media or without casamino acids struggled to power aerobic polymerizations. This latter result is consistent with previous reports showing that the absence of casamino acids significantly attenuates the specific growth rate of *S. oneidensis*[44]. Anaerobic respiration on Fe(III) in other *Shewanella* species is also slowed in the absence of these nutrients[45]. Similarly, removing casamino acids from our system decreased the polymerization rate under completely anaerobic conditions (Supplementary Fig. 17), but the effect was not as dramatic as under aerobic conditions. If growth rate and respiration are impaired, it is likely that aerobic respiration cannot compete effectively with oxygen diffusion to create the anaerobic environment required for polymerization. This is particularly problematic with monomers that negatively impact cell viability, since these may further impede respiration. Because aerobic polymerizations depend on the consumption of dissolved oxygen, we speculate that additional media-related polymerization activity differences are tied to *S. oneidensis* growth rate and relative flux through the TCA cycle. Under ideal aerobic conditions growing on lactate, *S. oneidensis* diverts a significant fraction of metabolic carbon flux (~50%) to the buildup of intermediates such as pyruvate and acetate[46,47]. Similar to *E. coli*, the inclusion of casamino acids and other nutrients may augment biomass synthesis and allow *S. oneidensis* cells to devote more resources to bioenergy generation via respiration, in addition to increasing their specific growth rate[48]. In our system, this translates to improved oxygen consumption and polymerization rates. Because our polymerization simultaneously leverages both aerobic and anaerobic metabolism, tuning these pathways in *S. oneidensis* could be used to further optimize polymerization activity[49,50].

Manipulating aerobic respiration rates in *E. coli* and other organisms to control dissolved oxygen has been a significant focus of metabolic engineering[50]. Applying similar strategies to *S. oneidensis* could expand the functional range of aerobic radical polymerizations by improving oxygen consumption rates. Once an anaerobic microenvironment is created, we showed that polymerization activity is governed by EET flux through the Mtr pathway. For example, we demonstrated that aerobic polymerization activity in *S. oneidensis* cultures is also dependent on the presence of the Mtr electron transfer pathway. A strain lacking MtrC and OmcA (Δ*mtrC*Δ*omcA*) displayed attenuated polymerization activity while additional

Mtr knockouts showed further reductions in polymerization rate, suggesting that MtrF is also an important contributor to Cu(II) reduction. Together, these results indicate that *S. oneidensis* controls polymerization by influencing the concentration of Cu(I) and K_{ATRP} via the expression of specific EET proteins. Thus, an alternative strategy for lowering K_{ATRP} and achieving better polymerization control is regulating EET flux through the controlled expression of Mtr pathway components. EET flux can be manipulated in other ways, such as removing hydrogenases[51], overexpressing flavins[52], or changing carbon sources. Similar to their use in microbial fuel cells, these strategies could be employed to increase or decrease EET flux to the metal catalyst over competing pathways. We have previously shown that the carbon source for *S. oneidensis* impacts polymerization rate under anaerobic conditions[13]. In this study, we used lactate in polymerization cultures involving *S. oneidensis*, but note that it can be transformed to metabolize glucose and other inexpensive carbon sources[53]. Alternatively, other facultative hosts containing both aerobic and EET pathways, such as different *Shewanella* species, Mtr-expressing *E. coli*, or *Vibrio natriegens* could be used in place of *S. oneidensis* to affect aerobic polymerizations[54-56]. Although our platform is potentially amenable to extensive optimization via metabolic engineering, the effectiveness of lyophilized and spent cells demonstrates its simplicity and reusability.

Overall, we showed that *S. oneidensis* enables aerobic radical polymerizations by consuming dissolved oxygen then activating an ATRP catalyst through its EET pathways. Polymerization was well-controlled, effective for a variety of monomers and metal catalysts, and could withstand repeated oxygen challenges. Finally, polymerization could be initiated using lyophilized *S. oneidensis* cells, improving the accessibility of our polymerization. Among electrogenic bacteria, *S. oneidensis* is unusual in that extracellular metal reduction is coupled to substrate-level phosphorylation to support cell growth[57]. Our results demonstrate how this unique hybrid of respiratory and fermentative metabolism, along with the facultative nature of *S. oneidensis*, can be used to address challenges in polymer synthesis and significantly expand the synthetic capabilities of biological systems.

Materials and Methods:

General Polymerization Conditions.

Prior to polymerizations, stock solutions of HEBIB (2.9 µL in 26.1 µL SBM containing casamino acids) and Cu-TPMA (200X stock from 8.9 mg $CuBr_2$ and 11.6 mg TPMA per 100 mL DMF) were prepared. Afterwards, a 1 mL polymerization reaction mixture was prepared as follows. In a sterile polypropylene culture tube, 60% w/w sodium lactate solution (2.85 µL), 1 M fumarate solution (40 µL), $OEOMA_{300}$ (28.6 µL), HEBIB (1.45 µL of stock solution), Cu-TPMA (5 µL of 200X DMF stock), and a balance of SBM with casamino acids, but lacking trace mineral mix, were mixed. Final concentrations were lactate (20 mM), fumarate (40 mM), monomer (100 mM), HEBIB (1 mM), and Cu-TPMA (2 µM). Polymerization was initiated by adding 10 µL of 100X cell stock (OD_{600} = 2.0 for anaerobic, OD_{600} = 20 for aerobic) to bring the final reaction volume to 1 mL and starting bacterial OD_{600} to 0.02 (anaerobic) or 0.2 (aerobic). Final reaction mixtures were incubated at 30 °C (*S. oneidensis*) or 37 °C (*E. coli*). Time points were aliquoted, diluted with deuterium oxide or GPC solvents, then flash frozen in liquid N_2. Aliquots were stored at −20

°C until analysis via NMR spectroscopy or GPC. Prior to GPC measurement, cells were spun down at 6000 x g from the water-soluble polymer solution. The polymer sample was loaded into dialysis tubing (MW cutoff: 1000–3000 Da) in corresponding dialysis buffer. After dialyzing for 2 hours, the buffer was replaced with fresh dialysis buffer and stirred overnight. Finally, the sample was removed from the dialysis bag, frozen at −80 °C overnight, then lyophilized.

Supplementary Material

Refer to Web version on PubMed Central for supplementary material.

Acknowledgements:

We thank Gauri Bora, Jennifer Imbrogno, Malgorzata Chwatko, and James Wagner for their experimental assistance. *S. oneidensis* knockouts were a generous gift from Jeffrey Gralnick. A.J.G. was supported through a National Science Foundation Graduate Research Fellowship (Program Award No. DGE-1610403). J.K. was supported through the Welch Foundation (Grant H-F-0001) during the Welch Summer Scholars Program. We gratefully acknowledge the use of facilities within the core microscopy lab of the Institute for Cellular and Molecular Biology, University of Texas at Austin. Hal Alper is thanked for the use of a BioLector Pro. Research reported in this publication was supported by the National Institute of General Medical Sciences of the National Institutes of Health under Award Number R35GM133640. The content is solely the responsibility of the authors and does not necessarily represent the official views of the National Institutes of Health. Additional research support was provided by the Welch Foundation (Grants F-1929 and F-1904) and by the National Science Foundation through the Center for Dynamics and Control of Materials: an NSF Materials Research Science and Engineering Center under Cooperative Agreement DMR- 1720595. NMR spectra were collected on a Bruker Avance III 500 funded by the NIH (Award 1 S10 OD021508-01) and a Bruker Avance III HD 400 funded by the NSF (Award CHE 1626211).

References:

1. Matyjaszewski K, Coca S, Gaynor SG, Wei M & Woodworth BE Controlled Radical Polymerization in the Presence of Oxygen. Macromolecules 31, 5967–5969 (1998).
2. Matyjaszewski K, Patten TE & Xia J Controlled “Living” Radical Polymerization. Kinetics of the Homogeneous Atom Transfer Radical Polymerization of Styrene. J Am Chem Soc 119, 674–680 (1997).
3. Chapman R, Gormley AJ, Herpoldt K-L & Stevens M Highly Controlled Open Vessel RAFT Polymerizations by Enzyme Degassing. Macromolecules 47, 8541–8547 (2014).
4. Chapman R, Gormley AJ, Stenzel MH & Stevens M Combinatorial Low-Volume Synthesis of Well-Defined Polymers by Enzyme Degassing. Angew Chem Int Ed 128, 4576–4579 (2016).
5. Oytun F, Kahveci MU & Yagci Y Sugar overcomes oxygen inhibition in photoinitiated free radical polymerization. J Polym Sci Part A Polym Chem 51, 1685–1689 (2013).
6. Enciso AE, Fu L, Russell AJ & Matyjaszewski K A Breathing Atom-Transfer Radical Polymerization: Fully Oxygen-Tolerant Polymerization Inspired by Aerobic Respiration of Cells. Angewandte Chemie Int Ed 57, 933–936 (2018).
7. Wang Y, Fu L & Matyjaszewski K Enzyme-Deoxygenated Low Parts per Million Atom Transfer Radical Polymerization in Miniemulsion and Ab Initio Emulsion. ACS Macro Lett 7, 1317–1321 (2018). [PubMed: 31815054]
8. Enciso AE et al. Biocatalytic “Oxygen-Fueled” Atom Transfer Radical Polymerization. Angewandte Chemie Int Ed 57, 16157–16161 (2018).
9. Pester CW et al. Engineering Surfaces through Sequential Stop-Flow Photopatterning. Adv Mater 28, 9292–9300 (2016). [PubMed: 27615382]
10. Narupai B et al. Simultaneous Preparation of Multiple Polymer Brushes under Ambient Conditions using Microliter Volumes. Angew Chem Int Ed 57, 13433–13438 (2018).

11. Gormley AJ et al. An Oxygen-Tolerant PET-RAFT Polymerization for Screening Structure-Activity Relationships. Angew Chem Int Ed 57, 1557–1562 (2018).
12. Yeow J, Chapman R, Gormley AJ & Boyer C Up in the air: oxygen tolerance in controlled/living radical polymerisation. Chem Soc Rev 47, 4357–4387 (2018). [PubMed: 29718038]
13. Fan G, Dundas C, Graham AJ, Lynd NA & Keitz BK Shewanella oneidensis as a living electrode for controlled radical polymerization. Proc National Acad Sci U.S.A. 115, 4559–4564 (2018).
14. Tang W & Matyjaszewski K Effect of Ligand Structure on Activation Rate Constants in ATRP. Macromolecules 39, 4953–4959 (2006).
15. Chmielarz P, Park S, Simakova A & Matyjaszewski K Electrochemically mediated ATRP of acrylamides in water. Polymer 60, 302–307 (2015).
16. Fantin M, Isse AA, Gennaro A & Matyjaszewski K Understanding the Fundamentals of Aqueous ATRP and Defining Conditions for Better Control. Macromolecules 48, 6862–6875 (2015).
17. Breuer M, Rosso KM & Blumberger J Electron flow in multiheme bacterial cytochromes is a balancing act between heme electronic interaction and redox potentials. Proc National Acad Sci U.S.A. 111, 611–616 (2014).
18. Shi L et al. Extracellular electron transfer mechanisms between microorganisms and minerals. Nat Rev Microbiol 14, 651–662 (2016). [PubMed: 27573579]
19. Silva TB et al. Hemoglobin and Red Blood Cells Catalyze Atom Transfer Radical Polymerization. Biomacromolecules 14, 2703–2712 (2013). [PubMed: 23739032]
20. Simakova A, Mackenzie M, Averick SE, Park S & Matyjaszewski K Bioinspired Iron-Based Catalyst for Atom Transfer Radical Polymerization. Angewandte Chemie Int Ed 52, 12148–12151 (2013).
21. Debuigne A, Poli R, Jérôme C, Jérôme R & Detrembleur C Overview of cobalt-mediated radical polymerization: Roots, state of the art and future prospects. Prog Polym Sci 34, 211–239 (2009).
22. Peng C-H, Yang T-Y, Zhao Y & Fu X Reversible deactivation radical polymerization mediated by cobalt complexes: recent progress and perspectives. Org Biomol Chem 12, 8580–8587 (2014). [PubMed: 25238612]
23. Granel C, Dubois, Jérôme R & Teyssié P Controlled Radical Polymerization of Methacrylic Monomers in the Presence of a Bis(ortho-chelated) Arylnickel(II) Complex and Different Activated Alkyl Halides. Macromolecules 29, 8576–8582 (1996).
24. Uegaki H, Kotani Y, Kamigaito M & Sawamoto M Nickel-Mediated Living Radical Polymerization of Methyl Methacrylate 1. Macromolecules 30, 2249–2253 (1997).
25. Ouchi M, Yoda H, Terashima T & Sawamoto M Aqueous metal-catalyzed living radical polymerization: highly active water-assisted catalysis. Polym J 44, 51–58 (2011).
26. Beliaev A et al. Global Transcriptome Analysis of Shewanella oneidensis MR-1 Exposed to Different Terminal Electron Acceptors. J Bacteriol 187, 7138–7145 (2005). [PubMed: 16199584]
27. Workman DJ, Woods SL, Gorby YA, Fredrickson JK & Truex MJ Microbial Reduction of Vitamin B_{12} by Shewanella alga Strain BrY with Subsequent Transformation of Carbon Tetrachloride. Environ Sci Technol 31, 2292–2297 (1997).
28. Amonette JE, Workman DJ, Kennedy DW, Fruchter JS & Gorby YA Dechlorination of Carbon Tetrachloride by Fe(II) Associated with Goethite. Environ Sci Technol 34, 4606–4613 (2000).
29. McKenna R & Nielsen DR Styrene biosynthesis from glucose by engineered E. coli. Metab Eng 13, 544–554 (2011). [PubMed: 21722749]
30. Kasai T, Kouzuma A, Nojiri H & Watanabe K Transcriptional mechanisms for differential expression of outer membrane cytochrome genes omcA and mtrC in Shewanella oneidensis MR-1. BMC Microbiol 15, 68 (2015). [PubMed: 25886963]
31. Geng J et al. Radical polymerization inside living cells. Nat Chem 11, 578–586 (2019). [PubMed: 30988414]
32. Niu J et al. Engineering live cell surfaces with functional polymers via cytocompatible controlled radical polymerization. Nat Chem 9, 537–545 (2017). [PubMed: 28537595]
33. Romero G et al. Protective Polymer Coatings for High-Throughput, High-Purity Cellular Isolation. ACS Appl Mater Inter 7, 17598–17602 (2015).

34. McCarthy B & Miyake GM Organocatalyzed Atom Transfer Radical Polymerization Catalyzed by Core Modified N -Aryl Phenoxazines Performed under Air. ACS Macro Lett 7, 1016–1021 (2018). [PubMed: 31827976]

35. Corrigan N, Rosli D, Jones J, Xu J & Boyer C Oxygen Tolerance in Living Radical Polymerization: Investigation of Mechanism and Implementation in Continuous Flow Polymerization. Macromolecules 49, 6779–6789 (2016).

36. Simakova A, Averick SE, Konkolewicz D & Matyjaszewski K Aqueous ARGET ATRP. Macromolecules 45, 6371–6379 (2012).

37. Sekar R & DiChristina TJ Microbially Driven Fenton Reaction for Degradation of the Widespread Environmental Contaminant 1,4-Dioxane. Environ Sci Technol 48, 12858–12867 (2014). [PubMed: 25313646]

38. Kotloski NJ & Gralnick JA Flavin electron shuttles dominate extracellular electron transfer by Shewanella oneidensis. Mbio 4, e00553–12 e00553-12 (2013). [PubMed: 23322638]

39. Batchelor R, Kwandou G, Spicer P & Stenzel M (−)-Riboflavin (vitamin B2) and flavin mononucleotide as visible light photo initiators in the thiol–ene polymerisation of PEG-based hydrogels. Polym Chem 8, 980–984 (2017).

40. Edwards M, White G & Norman M Redox Linked Flavin Sites in Extracellular Decaheme Proteins Involved in Microbe-Mineral Electron Transfer. Sci Rep 5, 11677 (2015). [PubMed: 26126857]

41. Ribelli TG, Lorandi F, Fantin M & Matyjaszewski K Atom Transfer Radical Polymerization: Billion Times More Active Catalysts and New Initiation Systems. Macromol Rapid Comm 40, e1800616 (2019).

42. Hau HH & Gralnick JA Ecology and Biotechnology of the Genus Shewanella. Annu Rev Microbiol 61, 237–258 (2007). [PubMed: 18035608]

43. Venkateswaran K et al. Polyphasic taxonomy of the genus Shewanella and description of Shewanella oneidensis sp. nov. Int J Syst Evol Micr 49, 705–724 (1999).

44. Tang YJ et al. Invariability of central metabolic flux distribution in Shewanella oneidensis MR-1 under environmental or genetic perturbations. Biotechnol Progr 25, 1254–1259 (2009).

45. Lovley D, Phillips E & Lonergan D Hydrogen and Formate Oxidation Coupled to Dissimilatory Reduction of Iron or Manganese by Alteromonas putrefaciens. Appl Environ Microb 55, 700–6 (1989).

46. Feng X, Xu Y, Chen Y & Tang YJ Integrating Flux Balance Analysis into Kinetic Models to Decipher the Dynamic Metabolism of Shewanella oneidensis MR-1. Plos Comput Biol 8, e1002376–12 (2012). [PubMed: 22319437]

47. Ishiki K & Shiigi H Kinetics of Intracellular Electron Generation in Shewanella oneidensis MR-1. Anal Chem (2019) doi:10.1021/acs.analchem.9b02900 .

48. Basan M et al. Overflow metabolism in Escherichia coli results from efficient proteome allocation. Nature 528, 99–104 (2015). [PubMed: 26632588]

49. Veit A, Polen T & Wendisch VF Global gene expression analysis of glucose overflow metabolism in Escherichia coli and reduction of aerobic acetate formation. Appl Microbiol Biot 74, 406–421 (2006).

50. Zhu J, Sánchez A, Bennett GN & San K-Y Manipulating respiratory levels in Escherichia coli for aerobic formation of reduced chemical products. Metab Eng 13, 704–712 (2011). [PubMed: 22001430]

51. Joshi K, Kane AL, Kotloski NJ, Gralnick JA & Bond DR Preventing Hydrogen Disposal Increases Electrode Utilization Efficiency by Shewanella oneidensis. Frontiers Energy Res 7, 95 (2019).

52. Yang Y et al. Enhancing Bidirectional Electron Transfer of Shewanella oneidensis by a Synthetic Flavin Pathway. ACS Synth Biol 4, 815–823 (2015). [PubMed: 25621739]

53. Choi D et al. Metabolically engineered glucose-utilizing Shewanella strains under anaerobic conditions. Bioresource Technol 154, 59–66 (2014).

54. Jensen HM, et al. Engineering of a synthetic electron conduit in living cells. Proc. Natl. Acad. Sci. U.S.A 107, 19213–19218 (2010).. [PubMed: 20956333]

55. Jensen HM, TerAvest MA, Kokish MG & Ajo-Franklin CM CymA and Exogenous Flavins Improve Extracellular Electron Transfer and Couple It to Cell Growth in Mtr-Expressing Escherichia coli. ACS Synth Biol 5, 679–688 (2016). [PubMed: 27000939]

56. Long CP, Gonzalez JE, Cipolla RM & Antoniewicz MR Metabolism of the fast-growing bacterium Vibrio natriegens elucidated by 13C metabolic flux analysis. Metab Eng 44, 191–197 (2017). [PubMed: 29042298]

57. Hunt K, Flynn J, Naranjo B, Shikhare I & Gralnick J Substrate-Level Phosphorylation Is the Primary Source of Energy Conservation during Anaerobic Respiration of Shewanella oneidensis Strain MR-1. J Bacteriol 192, 3345–3351 (2010). [PubMed: 20400539]

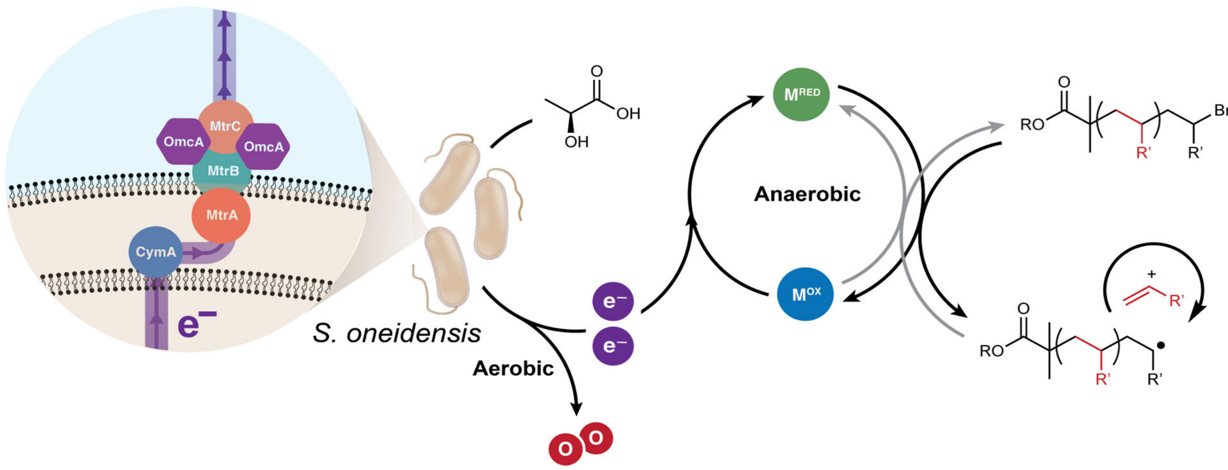

Figure 1.

Carbon oxidation in *S. oneidensis* is coupled to either oxygen reduction under aerobic conditions or extracellular electron transfer (EET) pathways under anaerobic conditions. At high cell densities, dissolved oxygen is depleted to create an *in situ* anaerobic environment where EET pathways are activated. Under anaerobic conditions, extracellular electron flux from the MtrCAB pathway in *S. oneidensis* MR-1 can be diverted to control the oxidation state of a transition metal polymerization catalyst through an atom-transfer radical polymerization mechanism. Polymerization rate and radical concentration are controlled by the equilibrium between oxidized (M^{OX}) and reduced (M^{RED}) metal catalyst.

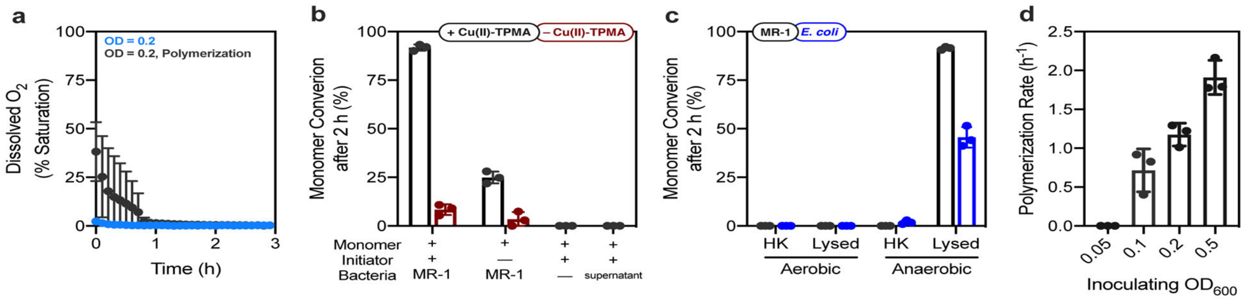

Figure 2.

S. oneidensis rapidly consumes dissolved oxygen and activates radical polymerization in cultures where no additional steps were taken to remove oxygen. (a) Dissolved oxygen in *S. oneidensis* MR-1 cultures growing in SBM and under typical polymerization conditions. Under both conditions, oxygen consumption outcompetes oxygen diffusion. (b) Effect of different biological and polymerization components on monomer ($OEOMA_{500}$) conversion under aerobic conditions. Monomer, initiator, catalysts, and *S. oneidensis* MR-1 are all required to achieve significant monomer conversion. (c) Monomer ($OEOMA_{500}$) conversion using heat-killed (HK) and lysed *E. coli* MG1655 or *S. oneidensis* MR-1 cells under anaerobic and aerobic conditions. Lysed cells release intracellular reductants that reduce Cu(II) to Cu(I), which activates polymerization. Under aerobic conditions, adventitious reductants and radicals are quenched by oxygen. Heat-killed cells do not result in polymerization under either condition since they neither consume oxygen or generate EET flux to reduce the metal catalyst. (d) Polymerization rate constants of $OEOMA_{500}$ using *S. oneidensis* MR-1 and Cu(II)-TPMA at varying inoculating OD_{600} under aerobic conditions. Data show mean ± SD of n = 3 replicates.

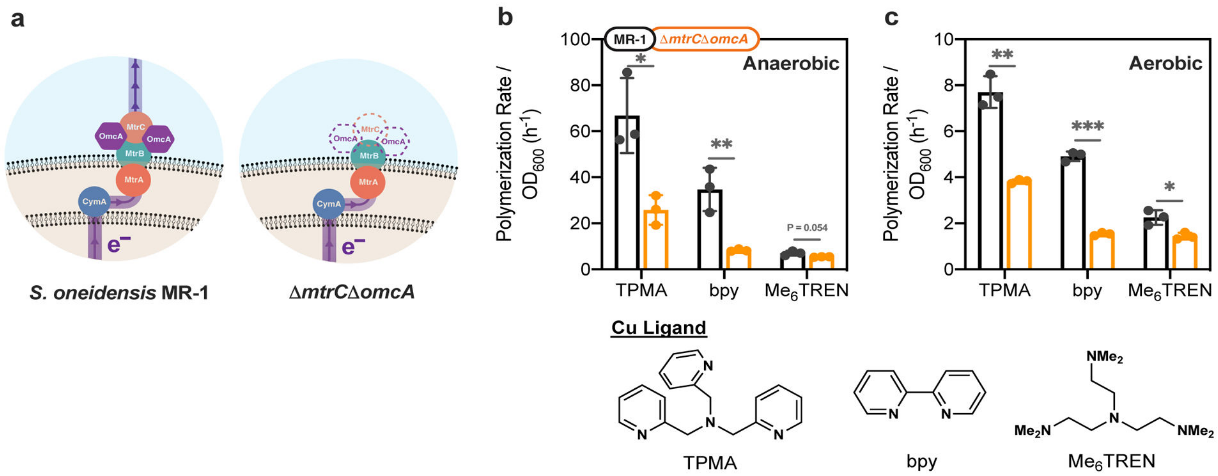

Figure 3.

S. oneidensis strain and Cu(II/I) ligand control polymerization kinetics under anaerobic and aerobic conditions. (a) Comparison of one extracellular electron transfer pathway in *S. oneidensis* MR-1 and an EET-deficient knockout (Δ*mtrC*Δ*omcA*) (b,c) Comparison of polymerization rate constants using *S. oneidensis* MR-1 or Δ*mtrC*Δ*omcA* and different Cu ligands normalized by initial cell inoculum in the polymerization mixture (OD_{600} = 0.02 for anaerobic, OD_{600} = 0.2 for aerobic). The Δ*mtrC*Δ*omcA* strain consistently showed decreased polymerization rate relative to wild-type *S. oneidensis*, consistent with the reduced level of EET flux expected for this knockout. The metal ligand affects Cu redox potential, Cu(I) stability, and overall polymerization activity. Data show mean ± SD of n = 3 replicates. *$p < 0.05$, **$p < 0.01$, ***$p < 0.001$.

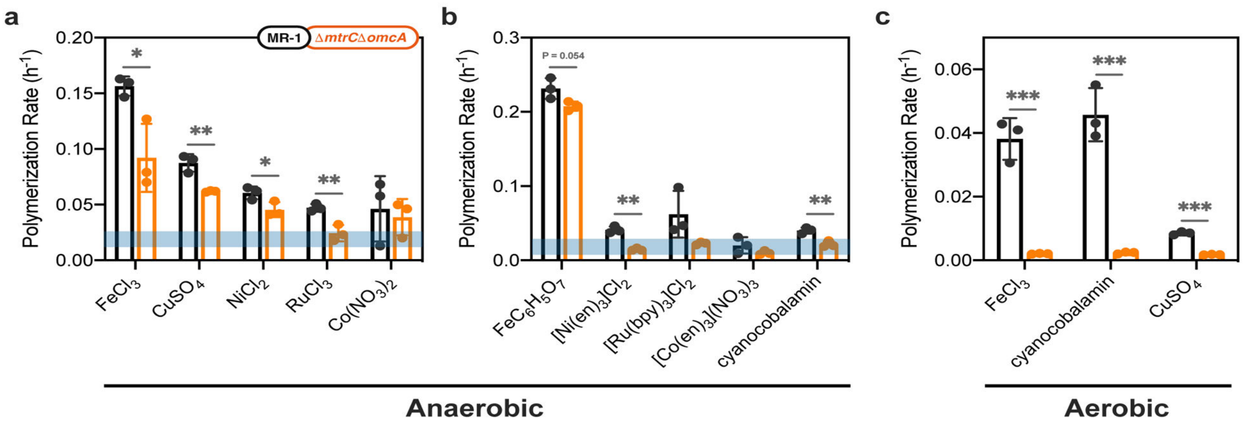

Figure 4.

Radical polymerization was effective for a variety of metal catalysts in addition to Cu. (a) Polymerization rate constants for different metal salts (2 μM) with EDTA and different *S. oneidensis* strains (initial OD_{600} = 0.02) under anaerobic conditions. The horizontal blue bar represents an estimated rate constant for the metal-free background polymerization (see Supplementary Fig. 9). (b) Polymerization rate constants for different metal complexes (2 μM) and *S. oneidensis* strains (initial OD_{600} = 0.02) under anaerobic conditions. (c) Polymerization rate constants for different metal catalysts (2 μM) and *S. oneidensis* strains (initial OD_{600} = 0.2) under aerobic conditions. Data show mean ± SD of n = 3 replicates. *$p < 0.05$, **$p < 0.01$, ***$p < 0.001$.

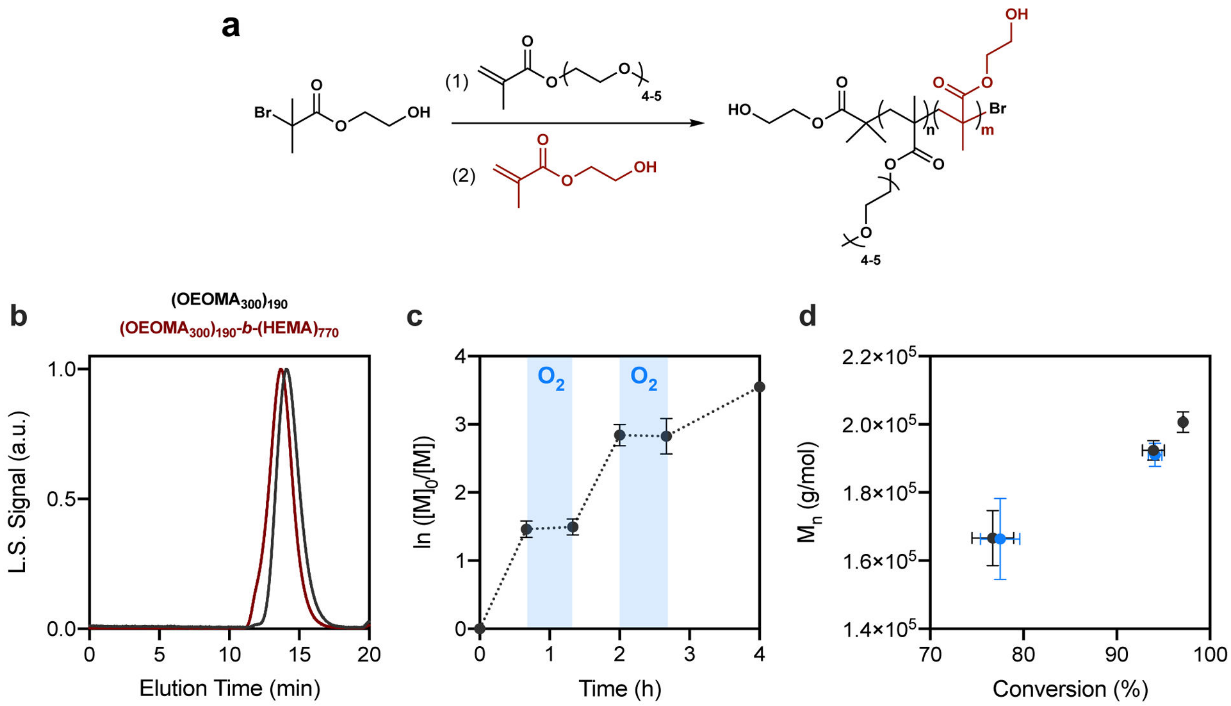

Figure 5.

Aerobic *S. oneidensis* polymerizations can be used to prepare block copolymers and restart automatically after multiple oxygen exposures. (a) Block copolymer of $OEOMA_{300}$ and HEMA synthesized under aerobic conditions with *S. oneidensis* MR-1. (b) Gel permeation chromatograph of homopolymer and block copolymer. (c) Polymerization kinetics in polymerization mixtures containing *S. oneidensis* with and without oxygen bubbling. Polymerization stops during oxygen bubbling as active Cu(I) catalyst is oxidized and *S. oneidensis* EET pathways are downregulated. After bubbling ceases, the polymerization automatically restarts with a similar rate as EET flux reduces Cu(II) to Cu(I). (d) Molecular weight of poly($OEOMA_{500}$) formed during oxygen bubbling experiment. Blue points represent polymers isolated during oxygen (1.5 h, 2.75 h) bubbling while black points represent polymers after bubbling ceased (0.75 h, 2.25 h, 4.25 h). The increase in molecular weight is consistent with polymerization restarting after oxygen bubbling stops. Data show mean ± SD of n = 3 replicates.

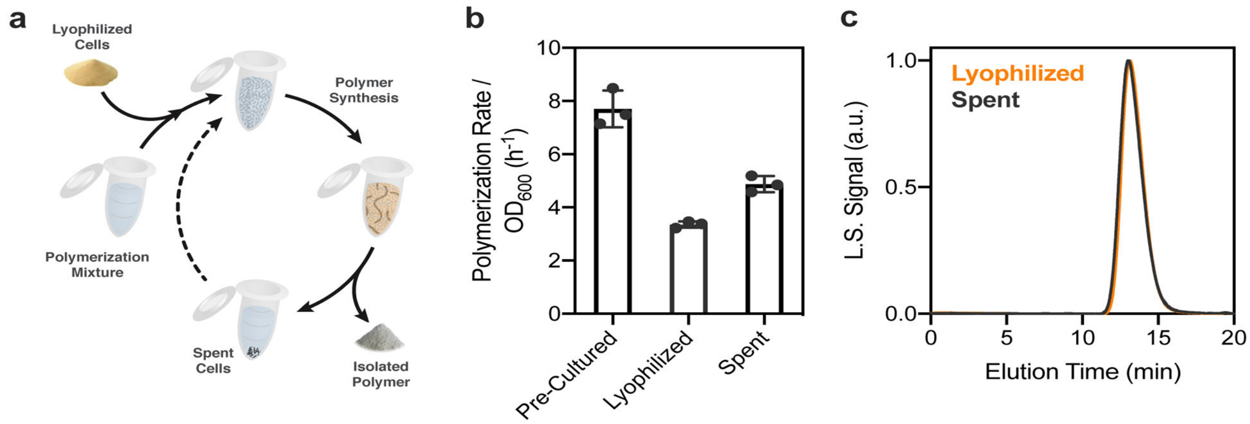

Figure 6.

Aerobic polymerizations are effective using lyophilized and spent *S. oneidensis* cells. (a) Reaction scheme for aerobic polymerizations using lyophilized and spent cells. Lyophilized cells were added to a polymerization mixture under aerobic conditions and sealed. Following polymerization, spent cells were collected via centrifugation, allowed to recover for 6 h in fresh media, then inoculated into a fresh polymerization mixture. (b) Polymerization rate constants starting from pre-cultured, lyophilized, and spent *S. oneidensis* MR- 1 cells. Normalized polymerization rates involving lyophilized cells were lower because higher inoculating cell densities were required to account for cell death during lyophilization. (c) GPC traces for poly(OEOMA$_{500}$) formed using lyophilized and spent cells. Unless otherwise indicated, data show mean ± SD of three replicates.

Table 1.

Monomer scope under anaerobic and aerobic polymerizations involving *S. oneidensis* MR-1. Yields are listed as percentages, followed by experimental M_n and Đ (PDI). Target M_n for monomer:initiator of 500:1 were pOEOMA$_{300}$ (150 kDa), pOEOMA$_{500}$ (250 kDa), pHEMA (65.1 kDa), pNIPAM (56.6 kDa), pDMAEMA (78.6 kDa), pMMA (50.1 kDa), PS (52.1 kDa). Averages and standard deviations were obtained from n = 3 replicates.

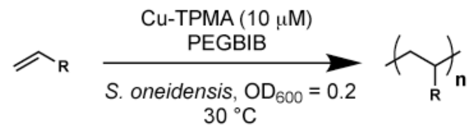

Monomer:	OEOMA$_{300}$	OEOMA$_{500}$	HEMA	MMA	DMAEMA	NIPAM	Styrene
	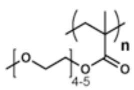	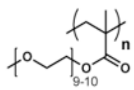	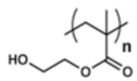	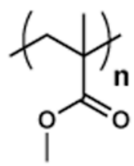	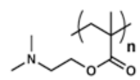	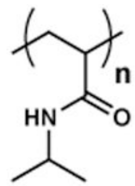	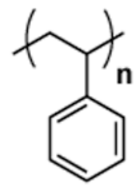
Anaerobic							
	82±10% 172±8 kDa Đ = 1.40(5)	95±2% 224±16 kDa Đ = 1.41(3)	86±2% 120±24 kDa Đ = 1.30(8)	96±2% 146±8 kDa Đ = 1.37(3)	83±4% 403±31 kDa Đ = 1.15(1)	98±2% 132±12 kDa Đ = 1.50(7)	14±2% 556±122 kDa Đ = 1.59(8)
Aerobic							
	67±10% 303±21 kDa Đ = 1.41(3)	96±2% 191 ±10 kDa Đ = 1.36(2)	77±10% 65±27 kDa Đ = 1.25(2)	8±3% 233±130 kDa Đ = 1.32(22)	-	88±14% 73±3 kDa Đ = 1.38(8)	11±1% 290±104 kDa Đ = 1.76(54)